Bull. Chem. Soc. Ethiop. **2025**, 39(3), 503-514.
DOI: https://dx.doi.org/10.4314/bcse.v39i3.9

ISSN 1011-3924
Printed in Ethiopia
Online ISSN 1726-801X

# TOWARDS THE COMPARISON SYNTHESIS OF $Fe_3O_4$ NANOCATALYSTS USING TWO DIFFERENT SYSTEMS IN FISCHER–TROPSCH PROCESS

Abdulqadier Hussien Al khazraji[1*], Ziad T. I. Alkayar[1], Maher Alwan Hussen[2] and Athraa Mohamed Rashed[1]

[1]Department of Chemistry, College of Education for Pure Science, University of Diyala, Diyala, Iraq
[2]The General Directorate for Education of Diyala, Diyala, Iraq

(Received July 3, 2024; Revised December 6, 2024; Accepted December 10, 2024)

**ABSTRACT**. Two types of nanocatalyst were synthesized using two different catalytic systems $Fe_3O_4$/ paraffin/polymethyl methacrylate ($Fe_3O_4$/pr/PMMA) and $Fe_3O_4$/paraffin/urotropine ($Fe_3O_4$/Pr/Uro) in Fischer–Tropsch synthesis (FTS) and downloaded in the slurry-bed reactor (SBR), their effect in the FTS performance and liquid hydrocarbons productivity were studied. The thermal decomposition method was used to prepare the nanoiron oxide nanocatalysts using the two systems. The results show that the two different systems affect the sizes of particle and gave nanoparticles with various sizes. The $Fe_3O_4$/paraffin/polymethyl methacrylate system nanocatalysts show good adsorption of syngas (CO:$H_2$), with high activity as compared to $Fe_3O_4$/paraffin/urotropin in the FTS system. In addition, the polymethyl methacrylate polymer has enhanced the interaction between $Fe_3O_4$ NPs and CO:$H_2$ molecule, leading improved syngas chemical adsorption and the formation of liquid hydrocarbons at all experimental temperatures, but with urotropin the conversion of CO was reduced when heated over 260 °C, and leading to lower the liquid hydrocarbons formation.

**KEY WORDS**: Fischer–Tropsch synthesis, Iron oxide nanoparticles, Polymethyl methacrylate, Urotropin

## INTRODUCTION

Iron was utilized as a catalyst by Fischer-Tropsch for the formation of hydrocarbons and fuels [1] [2]. Fischer-Tropsch synthesis (FTS) represents the area of catalytic hydrogenation in chemical processes which has been an interested field for many researchers, as demonstrated by the number of published reviews in the latest decade [3-5]. Over the two methods slurry and fixed; slurry reactor was utilized in a vast scope of chemical processes for the research and industrial scale [6, 7]. The most important step in the modification of FTS is the generation of highly active and selective catalysts [8, 9]. The effects of the polymer weight on the conversion of CO, liquid hydrocarbons productivity and the selectivity of the product were studied using a slurry bed reactor and the ($Fe_3O_4$/Pr/PEG) catalyst [10]. Al-Khazraji reported in a study the clear effect using copolymer on the nanocatalyst structure to an increase in the conversion CO and the formations of target product [11]. Sodium and sulfur modulated FeMnOx as catalysts have been employed for systematically investigate the influence of additives, which not only enhanced the CO conversion but also facilitate the olefin formation and suppressed the undesired methane formation [12]. Interestingly, using dispersion medium such as paraffin and polymers as stabilizers for iron nanoparticles synthesis highly affect the degree of productivity and selectivity of liquid hydrocarbons, as well as the stabilizers show a very good effect on the size of nanoparticles by producing the smallest one which is more useful in FTS [13]. In contrast, nano iron-based catalysts with different particle sizes were prepared by a co-precipitated method and the CO-TPD results revealed that large particle sizes of catalysts were not conducive to the adsorption of CO, and exhibited low activity of FTS [14]. Fe–Mn–Ce ternary nanocatalysts

*Corresponding authors. E-mail: abdulqadier.niama@uodiyala.edu.iq

supported on alumina granules that prepared by wetness impregnation method under vacuum and it has been evaluated as nanocatalysts in Fischer-Tropsch synthesis in the laboratory fixed bed microreactor. The optimum nanocatalyst composition for production of light olefins (C = 2 – C = 4) from synthesis gas is 75 wt% Fe – 20 wt% Mn – 5 wt% Ce, the maximum ratio of olefins/(methane + paraffin) and the best activity and selectivity belonged to the nanocatalyst which was calcined in static air at 500 °C for 7 hours [15]. The point of the present work is to obtain iron oxide nanocatalysts dispersed in two systems, paraffin/polymethyl methacrylate and paraffin/urotropin systems to study their effects on the dispersed iron oxide nanoparticles, activities, selectivity, and CO conversion in the FT process.

## EXPERIMENTAL

All compounds used were supplied by A.V. Topchiev Institute of Petrochemical Synthesis, Russian Academy of Sciences: Petroleum paraffin wax type P-2 code: (GOST 23683-89) which is a mixture of high molecular weight hydrocarbons of C18-C35, preferably aliphatic structure. Iron(III) nitrate nonahydrate ($Fe(NO_3)_3{\cdot}9H_2O$) type "extra pure" was purchased from manufacturer Scharlau Chemie S.A. Purified carbon monoxide (CO) supplied directly through pipelines from the decomposition of formic acid in the presence of sulfuric acid. Hydrogen ($H_2$) gas of technical grade A (GOST 3022-80) and Nitrogen ($N_2$) gas grade A (TU 6-21-39-96). Urotropin and polymethyl methacrylate polymer were supplied from A.V. Topchiev Institute of Petrochemical Synthesis, Russian Academy of Sciences.

After the synthesis of $Fe_3O_4$/paraffin/poly methyl methacrylate and $Fe_3O_4$/paraffin/urotropin, the samples were analysed by various analytical techniques like XRD, FE-SEM, AFM.

*Nanocatalysts preparation*. Iron oxide nanocatalysts were prepared using thermal decomposition method. Paraffin (100 mL) was heated up to 120 ºC, followed by addition of PMMA polymer or urotropin (10 g) and the reaction was heated up to 280 ºC under Argon. Then, freshly prepared solution of $Fe(NO_3)3.9H_2O$ (prepared by dissolving (43.23 g, 0.1 mol) in (20 mL) of distilled water) was added dropwise (5 mL/10 min) and the resultant solution were heated for 4 h at 280 ºC. The suspension nanocatalyst of $Fe_2O_3$/paraffin/poly methyl methacrylate and $Fe_2O_3$/paraffin/urotropin were obtained as inactive nanocatalysts. Figure 1 shows the parts of the $Fe_2O_3$/paraffin/polymethyl methacrylate and $Fe_2O_3$/paraffin/urotropin nanocatalyst preparation unit.

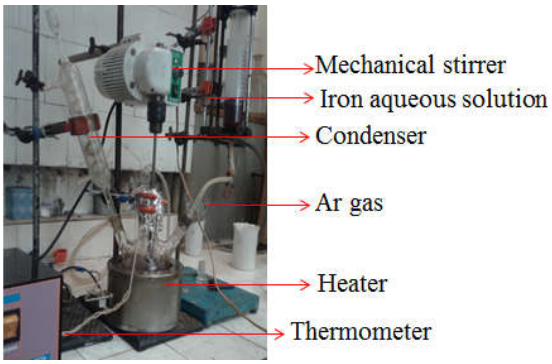


Figure 1. Synthesis of α-$Fe_2O_3$/paraffin/ poly methyl methacrylate and α-$Fe_2O_3$/ paraffin/urotropin nanocatalysts.

*Fischer Tropsch synthesis (FTS)*. The aged suspension iron oxide nanocatalyst was loaded in the slurry reactor and activated with CO gas at 300 °C for 24 hours to give the $Fe_3O_4$/paraffin/poly methyl methacrylate and $Fe_3O_4$/paraffin/urotropin as active nanocatalyst systems (equation 2). Then under the following conditions: The pressure of 2 MPa and syngas with a molar ratio of CO: $H_2$ = 1:1, in temperature range 220-320 ºC (the temperature increased gradually by 20 ºC interval every 12 hours over five days) the liquid hydrocarbons were formed. Figure 2 shows two steps, step one is the activation of $Fe_2O_3$/paraffin/polymethyl methacrylate and $Fe_2O_3$/paraffin/ urotropine nanocatalyst using CO gas to obtain $Fe_3O_4$/paraffin/polymethyl methacrylate, and step two is the download of $Fe_3O_4$/Pr/PMMA and $Fe_3O_4$/Pr/Uro nanocatalysts in the slurry reactor to liquid hydrocarbons production.

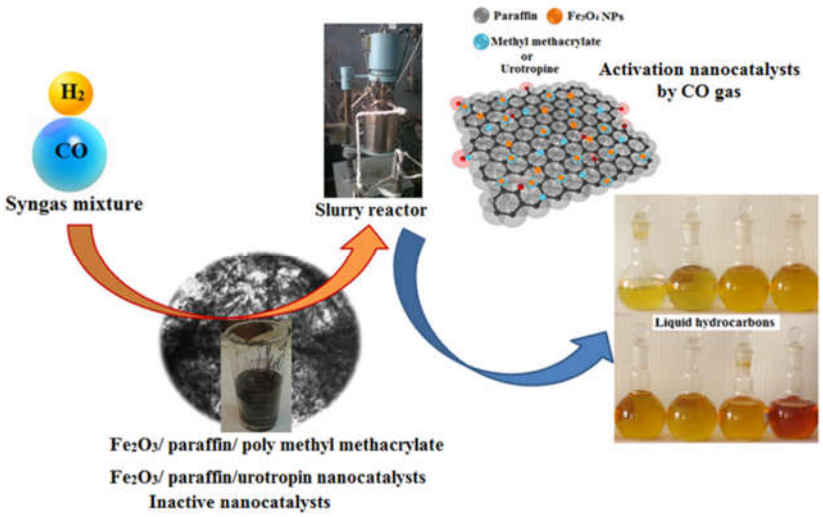


Figure 2. Synthesis of liquid hydrocarbons by FTS [10, 11].

*Particle size distribution*. The dynamic light scattering (DLS) technique was used to determine the nanoparticles size by Zetasizer Nano ZS instrument/Malvern. The sample has prepared by dissolving 0.01 g of the α-$Fe_2O_3$/paraffin/poly methyl methacrylate or paraffin/urotropine in 10 mL hexane and sodium dioctyl sulfosuccinate 5.0 wt% was added as a surfactant to stabilize the particles in dispersion.

*Analysis of liquid hydrocarbon Fischer-Tropsch synthesis products*

The liquid hydrocarbons that obtained during the Fischer-Tropsch synthesis process are contain a mixture of saturated and unsaturated aliphatic hydrocarbons of normal and isotropic structure. The amount of unsaturated hydrocarbons in the resulted products was calculated from the difference of sample volume before and after the treatment with concentrated sulfuric acid. The olefin content was determined using the following formula:

$$w_{ol,\%} = \frac{(V_1 - V_2)}{V_1} \cdot \rho \cdot 100\% \quad (1)$$

wol, % - mass fraction of olefins in the sample, $V_1$ - sample volume before treatment with sulfuric acid, $V_2$ - sample volume after treatment with sulfuric acid, ρ - average density of olefins (assumed equal to 0.7 g/mL).

The fractional composition of the hydrocarbon mixture was determined on the Crystallux-4000M chromatograph combined with a personal computer. The device was monitored and controlled using the special NetChromWin 2.1 program. The detector is a flame ionization detector. Gas feed rate: nitrogen - 30 mL/min, hydrogen - 25 mL/min, air - 250 mL/min. An OV-351 capillary column (50 m × 0.32 mm) was used for the determination. The sample volume is 0.1 μL. Temperature conditions: 50°C (2 min) – 50-260°C, 6°C/min – 260-270°C, 5°C/min – 270°C, 10 min. A typical chromatogram is shown in (Figure 8).

## RESULTS AND DISCUSSION

Tow nanocatalysts system were synthesized α-$Fe_2O_3$/paraffin/poly methyl methacrylate and paraffin/urotropine by thermal decomposition method (equation 2), then they were a reduction them by CO gas at 300 °C, 24 hours period to obtained $Fe_3O_4$/paraffin/poly methyl methacrylate and paraffin/urotropine nanocatalysts (equation 3).

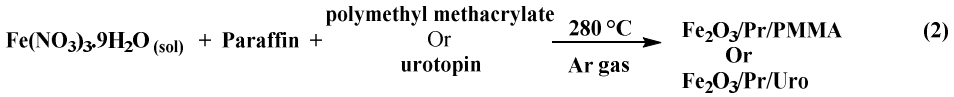


(2)

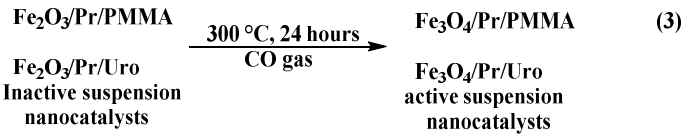


(3)

*The nanocatalyst systems characterization*. The nanocatalysts obtained by thermal decomposition were characterized using DLS, XRD, AFM and FE-SEM. XRD analysis confirmed the presence of $Fe_3O_4$ nanoparticles (magnetite phase). AFM and FE-SEM analysis revealed that $Fe_3O_4$/Pr/PMMA and $Fe_3O_4$/Pr/Uro have spherical shape with different and dispersed nanoparticles. Figure 3 illustrates the binding of iron oxide nanoparticles ($Fe_3O_4$) to the dispersion media of paraffin, polymer and urotropine.

*DLS analysis*. Attention is being focused on the paraffin/poly methyl methacrylate or urotropine surface matrix which contains iron oxide nanoparticles that produced using the method earlier [16]. In order to investigate the nanocatalysts nanoparticles size, three times have been selected to measure after adding the last drop of iron salt solution on the mixture suspension, the heating was stopped and the suspension was left to stirring under Ar gas, and immediately a sample was taken to measure the nanosize (at zero time). Then the mixture suspension was left to stir continuously with the temperature of the mixture suspension dropping, and after an hour of stirring another sample from the suspension was taken for the purpose of measuring the nanosize (at one hour), and again the measuring was repeated after two hours, until the process of preparing the nanocatalysts was completed. As a result, the change in nanosize was observed between the three selected times and the effect of preparation time and temperature on the size of the nanocatalyst. The distributions of the nanocatalyst particles are shown in Table 1. On the other hand, the two nanocatalyst systems containing PMMA and urotropin are exhibits a bimodal behaves over all preparation time (large and small size), Table 2. As a result, introducing synthetic polymer gave large nanoparticles size with narrow distribution.

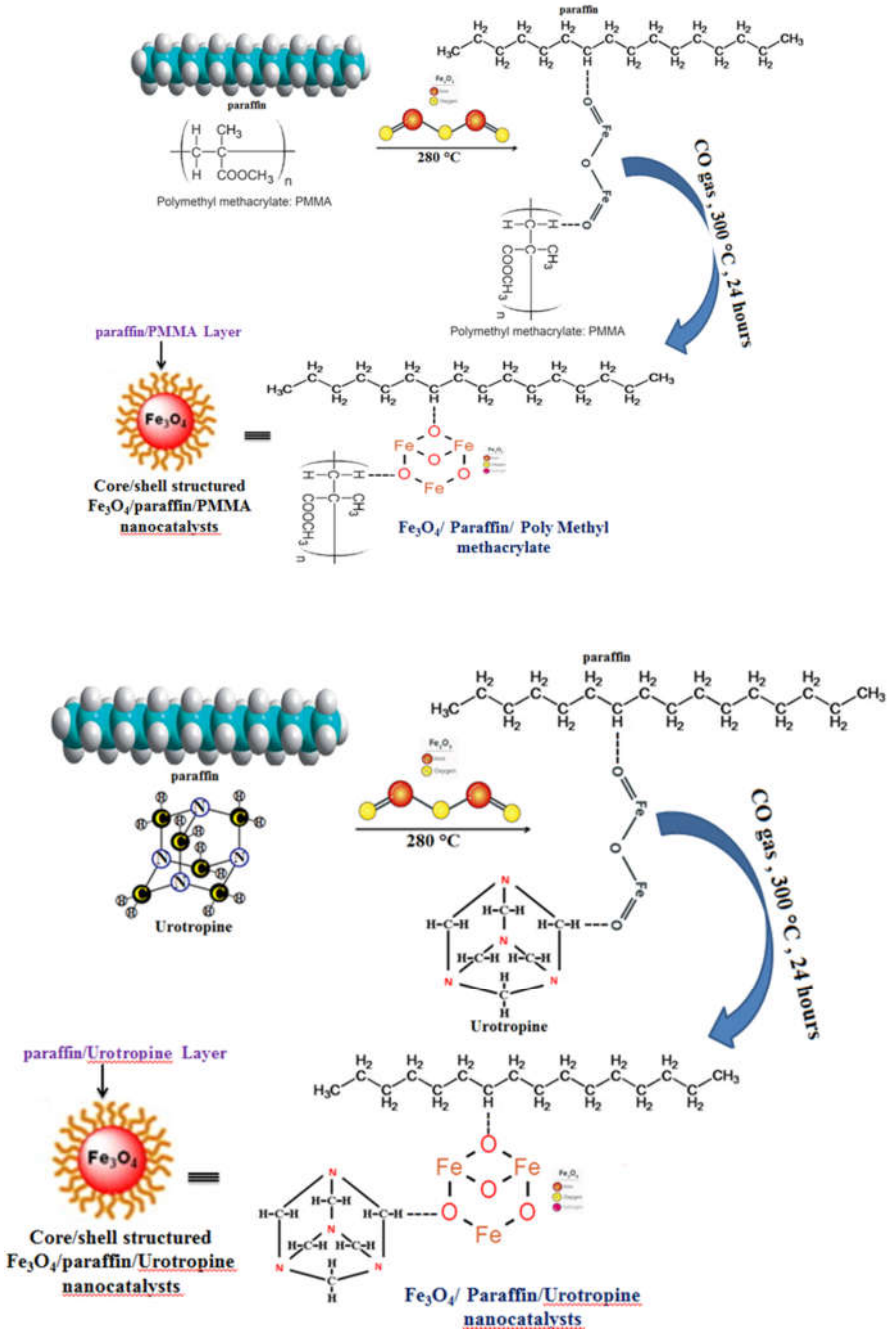


Figure 3. The chemical structure of paraffin, poly methyl methacrylate and urotropine bonded with $Fe_3O_4$ nanocatalyst.

Table 1. The time preparation (three time were chosen) effect on the nanoparticle size of the $Fe_3O_4$/paraffin/polymethyl methacrylate and $Fe_3O_4$/paraffin/urotropine nanocatalysts.

| Nano-catalyst | Particles size changes in (nm) of catalyst system over time | | | | | |
|---|---|---|---|---|---|---|
| | nm at 0*h | Content % nano | nm at 1* hour | Content % nano | nm at 2* hours | Content % nano |
| $Fe_3O_4$/Pr/ PMMA | 257 | 14 | 694 | 88 | 270 | 12 |
| | 866 | 86 | 1247 | 12 | 834 | 88 |
| $Fe_3O_4$/Pr/ Uro | 145 | 7 | 134 | 11 | 171 | 19 |
| | 765 | 93 | 626 | 89 | 664 | 81 |

*0 hour: After final drop added and full-size precursor solution under argon. *1 hour: After 1 hour under Argon. *2 hour: After 2 hour under argon.

Table 2. The DLS data of the nanocatalysts particle size.

| Nano-catalyst | Z-Average (r. nm) | Peak 1 | | | Peak 2 | | |
|---|---|---|---|---|---|---|---|
| | | Diam.(nm) | % Intensity | Width (nm) | Diam. (nm) | % Intensity | Width (nm) |
| $Fe_3O_4$/Pr/PMMA | 168.1 | 191 | 98.4 | 79.13 | 2596 | 1.6 | 239.6 |
| $Fe_3O_4$/Pr/ Uro | 464.1 | 919.4 | 83.4 | 481.1 | 138.9 | 16.6 | 44.04 |

The results of DLS showed that the distrbution nanoparticlels size of $Fe_3O_4$/Pr/PMMA and $Fe_3O_4$/Pr/Uro nanocatalysts was different. Dispersion the $Fe_3O_4$ nanoparticles with PMMA gave bimodal with large size and their size reached 191-2596 nm. While dispersion the $Fe_3O_4$ nanoparticles with urotropine gave to nanoparticles with small size which was about 138.9-919.4 nm.

*XRD analysis*. The XRD spectrum for $Fe_3O_4$/paraffin/PMMA and $Fe_3O_4$/paraffin/urotropine nanocatalyst clearly shows the major diffraction peaks of iron oxide ($Fe_3O_4$ phase) nanoparticles is predominate, Figure 4 [17, 18]. The diameter of synthesized $Fe_3O_4$ nanoparticle has calculated via Debye-Scherrer equation. The diffraction peaks in $Fe_3O_4$ NPs are basically the same as the ones nearly in the two systems. Generally, the addition of PMMA or urotropine compound will set up new diffraction peaks. However, the XRD investigation indicates that the positions of the diffractive peaks are basically similar. However, based on the obtained result indicates that there was no complete crystal transformation of $Fe_3O_4$ NPs during the FTS reaction and because of that the α-$Fe_2O_3$ might be amorphous and unconverted complete to $Fe_3O_4$ during the reduction process by carbon monoxide in the activation process of nanocatalysts. Moreover, we believe that the iron oxide amorphous is referring to δ-FeOOH. The average sizes were calculated using Scherer equation for both $Fe_3O_4$/paraffin/polymethyl methacrylate and $Fe_3O_4$/paraffin/urotropine systems and gave 30.87 nm and 29.58, respectively.

*Atomic force microscopy analysis (AFM)*. The nanometer-resolution three-dimensional images can be provided using atomic force microscopy (AFM). However, the AFM for $Fe_3O_4$/paraffin/methyl methacrylate system revealed highly textured surface morphology, such feature plays a significant role for the activity and CO conversion selectivity [19], Figure 5a. Whereas for urotropine (hexamethylenetetramine) which is a heterocyclic organic compound with the formula of $(CH_2)_6N_4$ has a compacted cage-like structure similar to adamantine, Figure 5b. We think that the presence of urotropine in the reaction medium behaved as a base due to the unshared paired electrons on nitrogen, which tends to affiants with iron orbitals and expect to activate the site of iron nanoparticals of the catalyst. Such sort of coordination brings the catalyst surface to a fully covered or in another word fully poisoned surface, even if it looks smooth and low feature surface as shown in figure 7 b, such reason can explain the low yield.

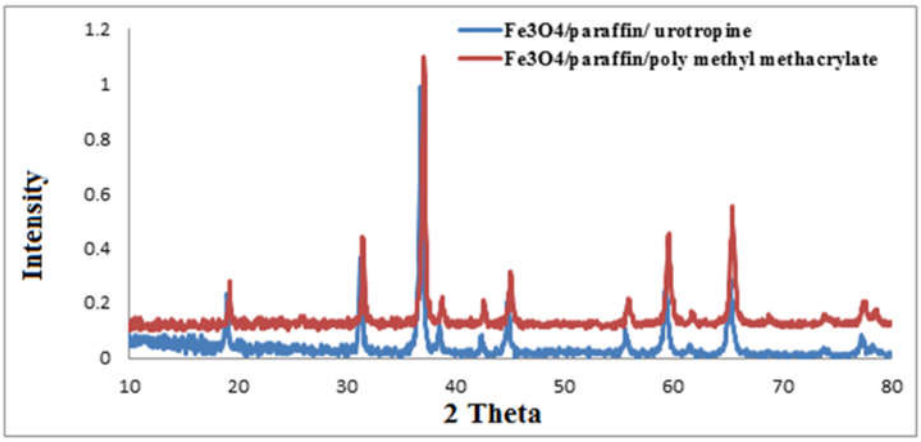


Figure 4. XRD patterns of $Fe_3O_4$/Pr/PMMA, and $Fe_3O_4$/Pr/Uro nanocatalyst.

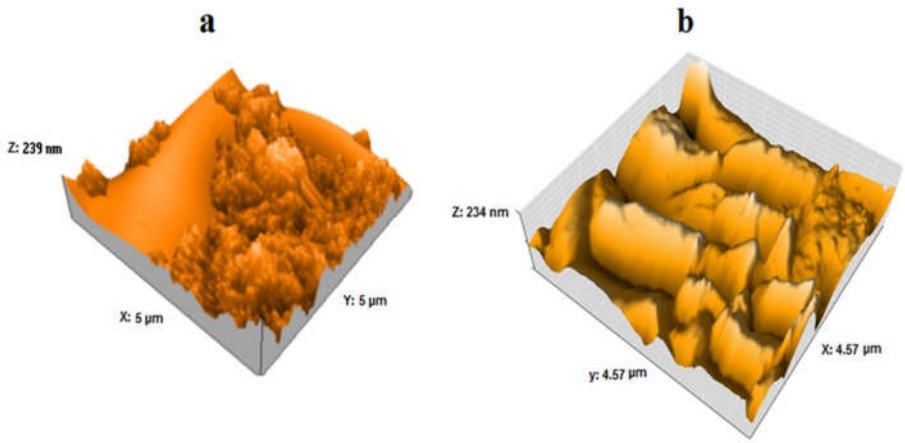


Figure 5. AFM images for (a) $Fe_3O_4$/Pr/PMMA and (b) $Fe_3O_4$/Pr/Uro nanocatalysts.

*FE-SEM image*. The FE-SEM images for the $Fe_3O_4$/Pr/PMMA and $Fe_3O_4$/Pr/Uro nanocatalysts are illustrated in Figure 6a and b, respectively. Regard morphology of the surfaces for the prepared nanocatalysts appeared unregulated and have more non uniform or wavy laminated surface with great in their surface depth with sharp tips. Increasing the heat leads to dissolve the paraffin and that resulted in leaving the surface of the stabilizing polymer, hence the polymer as a matrix can provide well distribution of iron oxide nanoparticles on the surface. The image for $Fe_3O_4$/Pr/PMMA nanoatalysts shows that the average size of nanoparticles was 67.12 nm with irregular shape as a result of agglomerations of the amorphous polymer (Figure 6a). While for $Fe_3O_4$/Pr/Uro nanocatalyst (Figure 6b) the image shows that the average size of nanoparticles was 45.43 nm with less decrease in the size of nanoparticles, nanocatalyst gave a heterogeneous plates shaped and nanoparticles non-aggregated [20]. We believe that the paraffin with polymer as a matrix can provide well distribution of iron oxide nanoparticles on the surface compare as paraffin with urotropine, this of course would have a great impact on the efficiency, selectivity liquid

hydrocarbons (C+5) and CO conversion, and this confirmed that the system is better than the system based on urotropine compound. Hence, the addition of PMMA polymer to the $Fe_3O_4$/Paraffin system, initiates the surface to be more homogenous leading to better dispersion.

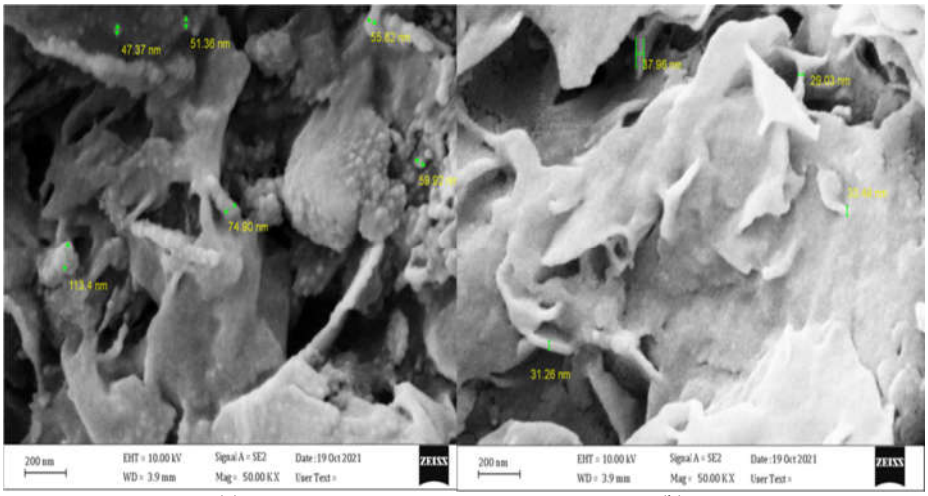


(a) (b)

Figure 6. FE-SEM image (a) $Fe_3O_4$/Pr / PMMA, and (b) $Fe_3O_4$/Pr/Uro nanocatalyst.

*FTS reaction*. The best formation of liquid hydrocarbons and CO conversion were achieved by suspended nanocatalysts at a temperature range of 220-320 ºC in the FTS Figure 7(a-e) high formations of methane and $CO_2$ gases. In the sample based on PMMA, the selectivity toward the liquid hydrocarbon target products has dropped dramatically from 78% to 23% with an increase the temperature up to 220-320 ºC. While those toward C5+ (liquid hydrocarbon) remain unchanged in the sample that contains Urotropine Figure 9b. This indicates that the rate of the reaction of the nanocatalysts could greatly improve by the addition of $Fe_3O_4$ nanoparticles over the polymer as compared to Urotropine CO conversion (XCO) and C5+ selectivity was calculated by the following equations (4) and (5) [21]:

$$\text{CO conversion} = \frac{Moles\ CO_{in} - Moles\ CO_{out}}{Moles\ CO_{in}} \times 100 \quad (4)$$

$$\text{Selectivity of j product \%} = \frac{\text{Moles of j product}}{Moles\ CO_{in} - Moles\ CO_{out}} \times 100 \quad (5)$$

The temperature rise seemed affecting the catalytic performance for C5+ selectivity of FTS reactions for both nanocatalysts. Both two nanocatalysts are found to give remarkably high C5+ selectivity with reduced temperature at 220 °C, but at high temperature at 320 °C give less C5+ selectivity, which displaying a declining trend with increase in temperature. The analysis of liquid hydrocarbons confirmed that the structure of component in the catalysts also has the fractional composition effect and the composition of liquid production (n-paraffin, iso-paraffin and alkene), which exist in the organic layer, Figure 8a and b.

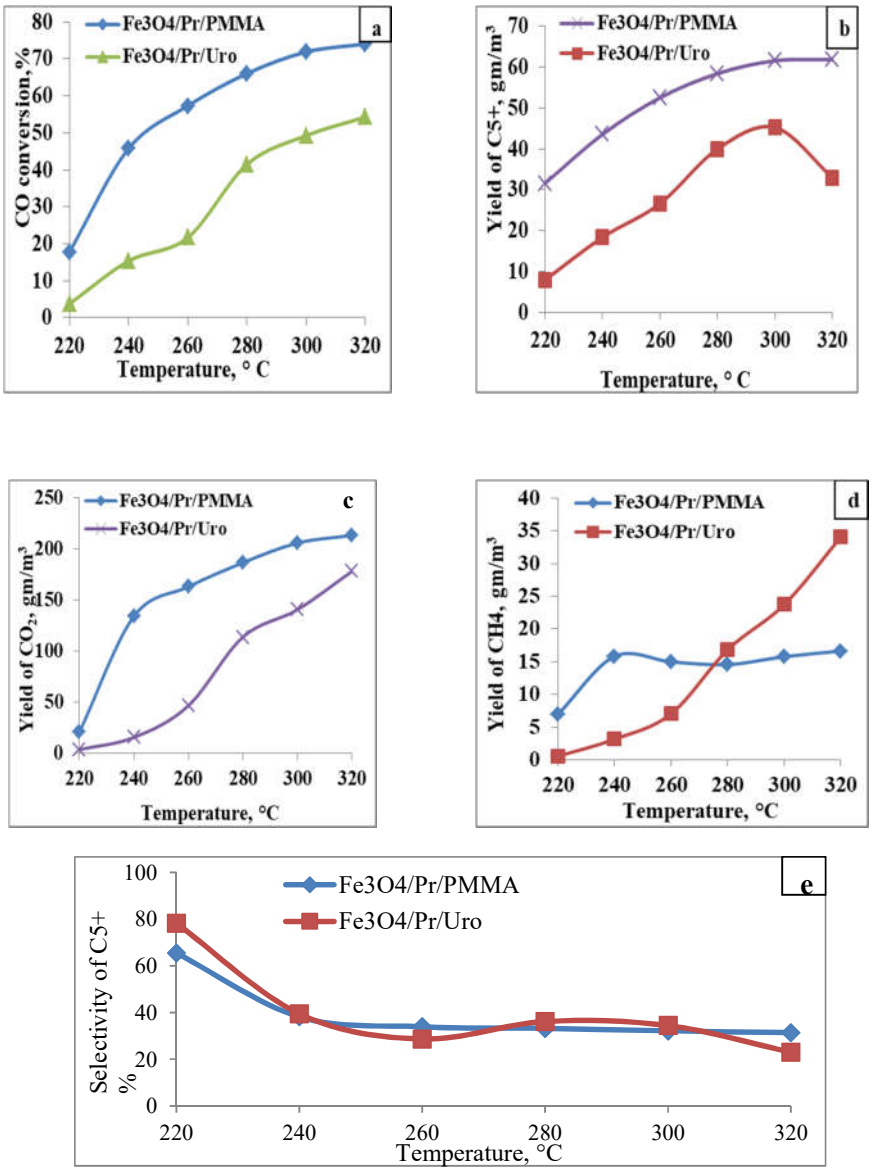


Figure 7. FTS result (a) CO conversion, (b) formation of liquid hydrocarbon (C5+), (c) $CO_2$ gas yield, (d) $CH_4$ gas yield, and (e) C5+ selectivity over $Fe_3O_4$/Pr/PMMA and $Fe_3O_4$/Pr/Uro nanocatalysts.

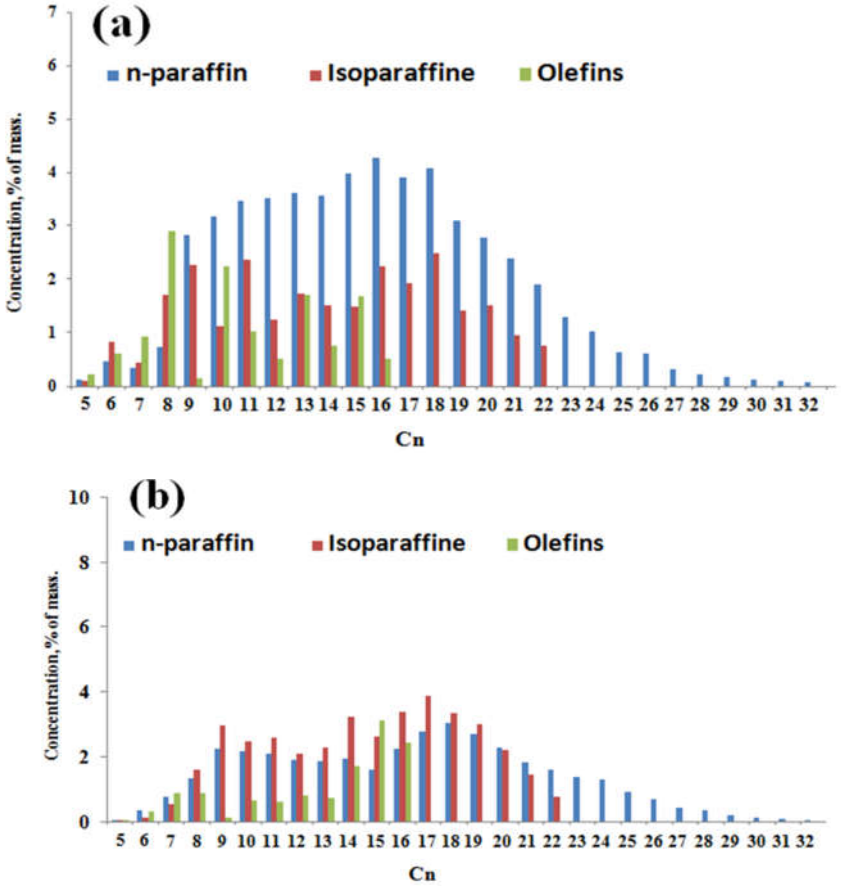


Figure 8. The composition of liquid hydrocarbons produced in the presence of: (a) $Fe_3O_4$/Pr /PMMA, and (b) $Fe_3O_4$/Pr/Uro nanocatalysts.

## CONCLUSION

Two types of nanocatalysts the $Fe_3O_4$/paraffin/polymethyl methacrylate and $Fe_3O_4$/paraffin/urotropin were prepared successfully using thermal decomposition method, and which were used to investigate the activity and the selectivity behavior during Fischer–Tropsch synthesis (FTS) in a slurry reactor. The obtained results were compared to each other in order to study the additives effect. However, the result indicates that the $Fe_3O_4$/paraffin/polymethyl methacrylate is better for CO conversions and liquid hydrocarbons formation of nanocatalysts, but the $CO_2$ gas formation was not good as compared to $Fe_3O_4$/paraffin/urotropine nanocatalyst particularly in the range temperature of 280-320 ºC. The nanocatalyst based on PMMA gave high selectivity of liquid hydrocarbons at 220 ºC. XRD analysis confirmed the presence of iron oxide $Fe_3O_4$ nanoparticles with average size of nanocatalysts 30.87 nm and 29.58 nm for $Fe_3O_4$/paraffin/polymethyl methacrylate and $Fe_3O_4$/Paraffin/Urotropine systems, respectively. AFM analysis indicates the existence of a winding surface which provides active sites to help the contact gas as compared to the surface of the catalyst on the basis of urotropine, since it is smooth

and does not help the contact gases. The average size of nanoparticles was 67.12 nm which was confirmed by the FE-SEM image of $Fe_3O_4$/Pr/PMMA nanocatalyst with irregular shape resulting from agglomerations of the amorphous polymer and the nanoparticles average size $Fe_3O_4$/Pr/Uro nanocatalyst was 45.43 nm.

## ACKNOWLEDGEMENTS

We would like to thank; A.V. Topchiev Institute of Petrochemical Synthesis, Russian Academy of Sciences. Since the work have performed using their equipment and supported via the President of Russian Federation.

## REFERENCES

1. Nasser, A.; El-Bery, M.; ELnaggar, H.; Basha, K.; El-Moneim, A. Selective conversion of syngas to olefins via novel Cu-promoted Fe/RGO and Fe–Mn/RGO Fischer–Tropsch catalysts: Fixed-bed reactor vs slurry-bed reactor. *ACS Omega* **2021**, 6, 31099-31111.
2. Han, Z.; Qian, W.; Ma, H.; Wu, X.; Zhang, H.; Sun, Q.; Ying, W. Study of the Fischer–Tropsch synthesis on nano-precipitated iron-based catalysts with different particle sizes. *RSC Adv.* **2020**, 10, 42903-42911.
3. Chae, Ho.; Kim, J.; Lee, S.; Kim, H.; Jo, S.; Ryu, J.; Kim, T.; Lee, Ch.; Kim, S.; Kang, H.; Kim, Ja.; Park, M. Catalytic technologies for CO hydrogenation for the production of light hydrocarbons and middle distillates. *Catal.* **2020**, 10, 99.
4. Teimouri, Z.; Abatzoglou, N.; Dalai, K. Kinetics and selectivity study of Fischer–Tropsch synthesis to C5+ hydrocarbons: A review. *Catal.* **2021**, 11, 330.
5. Ten Have, C.; Weckhuysen, M. The active phase in cobalt-based Fischer-Tropsch synthesis. *Chem. Catal.* **202**1, 1, 339-363.
6. Akay, G.; Zhang, K.; Al-Harrasi, S.; Sankaran, M. Catalytic plasma Fischer-Tropsch synthesis using uierarchically connected porous $Co/SiO_2$ catalysts prepared by microwave-induced Co-assembly. *Ind. Eng. Chem. Res.* **2020**, 59, 12013-12027.
7. Shafer, D.; Gnanamani, K.; Graham, M.; Yang, J.; Masuku, M.; Jacobs, Gary.; Davis, H. Fischer–Tropsch: Product selectivity–the fingerprint of synthetic fuels. *Catal.* **2019**, 9, 259.
8. Zhao, Z.; Lu, W.; Feng, C.; Chen, X.; Zhu, H.; Yang, R.; Dong, W.; Zhao, M.; Lyu, Y.; Liu, T. Increasing the activity and selectivity of Co-based FTS catalysts supported by carbon materials for direct synthesis of clean fuels by the addition of chromium. *J. Catal.* **2019**, 370, 251-264.
9. Zhu, C.; Gamliel, P.; Valla, A.; Bollas, M. Applied catalysis B: Fischer-Tropsch synthesis in monolith catalysts coated with hierarchical ZSM-5. *Appl. Catal. B: Environ.* **2021**, 284, 119719.
10. Al khazraji, A.; Alkayar, Z.; Rashed, A.; Fahmi, A. Effect of polymer weight on the Fischer-Tropsch synthesis kinetics over the iron oxide/paraffin/polymer systems as nanocatalysts. *Passer J.* **2024**, 6, 381-389.
11. Al-Khazraji, A. Influence of iron nano Co-polymer catalysts on the liquid hydrocarbons production in the synthesis Fischer Tropsch. *JGPT* **2019**, 11, 827-834
12. Yang, X.; Yang, J.; Wang, Y.; Zhao, T.; Ben, H.; Li, X.; Holmen, A.; Huang, Y.; Chen, De. Promotional effects of sodium and sulfur on light olefins synthesis from syngas over iron-manganese catalyst. *Appl. Catal. B: Environ.* **2022**, 300, 120716.
13 Delgadoa, A.; Claver, C.; Castillonc, S.; Curulla-Ferre, D.; Ordomskye,V.; Godard, C. Effect of polymeric stabilizers on Fischer–Tropsch synthesis catalyzed by cobalt nanoparticles supported on $TiO_2$. *J. Mol. Catal. A: Chem.* **2016**, 417, 43-52.
14 Han, Z.; Qiana, W.; Maa, H.; Wua, X.; Zhang, H.; Sunb, Q.; Ying, W. Study of the Fischer–Tropsch synthesis on nano-precipitated iron-based catalysts with different particle sizes. *RSC Adv.* **2020**, 10, 42903-42911.

15 Roknabadi, R.; Mirzaei, A.; Atashi, H. Assessment of composition and calcination parameters in Fischer-Tropsch synthesis over Fe–Mn–Ce/γ-$Al_2O_3$ nanocatalyst. *Oil Gas Sci. Technol. - Rev. IFP Energies Nouvelles* **2021**, 76, 11.
16 Al khazraji, A.; Ghalib, A.; Sahar, H. The effect of the polymer type in the three-phases Fischer-Tropsch synthesis catalyzed by suspended iron nanocatalysts. *Mediterr. J. Chem.* **2019**, 9, 363-370.
17 Saeed, M.; Usman, M.; Muneer, M.; Akram, N.; Haq, ul.; Tariq, M.; Akram, F. Synthesis of ag-$Fe_3O_4$ nanoparticles for degradation of methylene blue in aqueous medium. *Bull. Chem. Soc. Ethiop.* **202**0, 34, 123-134.
18 Hamadamin, Sh.; Anwer, S.; Abdulkareem, P.; Sdiq, K. Biogenic synthesis of ferrous(III) oxide and $Fe_3O_4/SiO_2$ using chlorella sp. and its adsorption properties of water contaminated with copper(II) ions. *Bull. Chem. Soc. Ethiop.* **2022**, 36, 585-596.
19 Ngema, B.; Farahani, D.; Raseale, S.; Fischer, N.; Mohamed, S.; Singh, S.; Friedrich, B. In situ construction of a highly active surface interface for a $Co_3O_4/ZrO_2$ catalyst enhancing the CO-PrOx activity. *Surf. Interf.* **2023**, 38, 102826.
20. Lee, J.; Lu, Q.; Lee, J.; Choi, H. Polymer-magnetic composite particles of $Fe_3O_4$/Poly(o-anisidine) and their suspension characteristics under applied magnetic fields. *Polymers* **2019**, 11, 219.
21. Nisa, M.; Chen, Y.; Li, X.; Jiang, X.; Li, Z. Modulating C5+ selectivity for Fischer-Tropsch synthesis by tuning pyrolysis temperature of MOFs derived Fe-based catalyst. *JTICE* **2022**, 131, 104170.